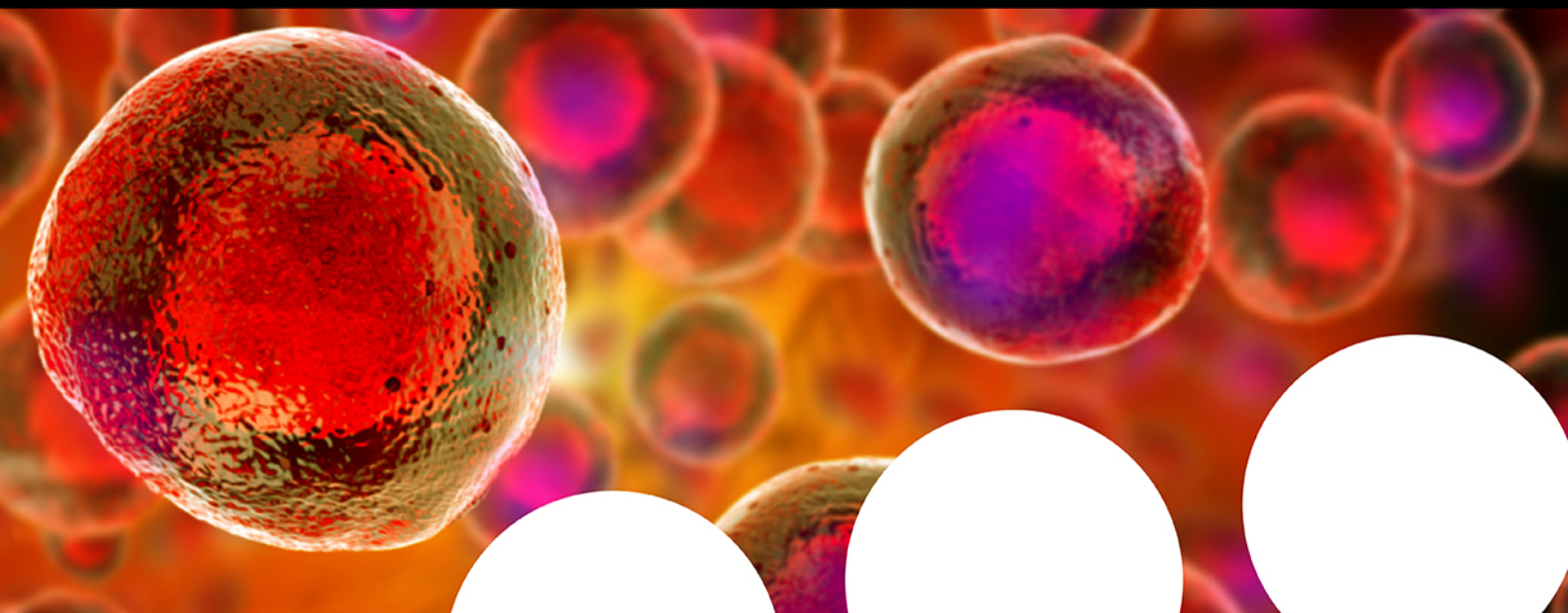


# Your research is important and needs to be shared with the world



## Benefit from the Chemistry Europe Open Access Advantage

- Articles published open access have higher readership
- Articles are cited more often than comparable subscription-based articles
- All articles freely available to read, download and share.

**Submit your paper today.**



[www.chemistry-europe.org](http://www.chemistry-europe.org)

# Catechol-Functionalized Carbon Nanotubes as Support for Pd Nanoparticles: a Recyclable System for the Heck Reaction

Alessandro Mercadante,<sup>[a]</sup> Vincenzo Campisciano,<sup>\*,[a]</sup> Anthony Morena,<sup>[a, b]</sup> Laura Valentino,<sup>[a]</sup> Valeria La Parola,<sup>[c]</sup> Carmela Aprile,<sup>[b]</sup> Michelangelo Gruttadauria,<sup>[a]</sup> and Francesco Giacalone<sup>\*,[a]</sup>

*Dedicated to Prof. Cesare Gennari on the occasion of his 70th birthday*

Carbon nanotubes have been covalently functionalized with catechol moieties through the formation of the corresponding aryl radicals obtained by reacting 4-aminocatechol with isoamyl nitrite. The functionalized multiwalled carbon nanotubes have been in turn used to immobilize Pd(II) ions on its surface forming catechol-Pd complexes, which were reduced to Pd nanoparticles (NPs). The so-obtained hybrid material has been characterized by means of thermogravimetric analysis coupled with differential scanning calorimetry (TGA-DSC), X-ray photo-

electron spectroscopy (XPS) and transmission electron microscopy (TEM). This latter technique allowed to estimate the nanoparticle size ( $5.7 \pm 2.8$  nm) whereas a palladium loading of 20.3 wt % has been found by inductively coupled plasma optical emission spectroscopy (ICP-OES). The carbon nanotube-catechol-Pd hybrid was used as catalyst in two C–C coupling reactions, namely Suzuki and Heck reactions, resulting recyclable for at least 9 times in the latter process. During the reuse Pd nanoparticles increase their dimension to  $19.3 \pm 11.7$  nm.

## Introduction

Carbon nanotubes (CNTs), due to their numerous applications in a plethora of fields, are at the focus of a huge amount of research. However, despite the well-known properties of this allotropic form of carbon, such as high chemical and thermal stability, mechanical strength, and excellent electrical and thermal conductivity, the poor processability of pristine CNTs can hinder their widespread utilization. The strong van der Waals interactions are responsible for the formation of ropes

and bundles which makes CNTs poorly dispersible in most media. This lack of solubility/dispersibility can be circumvented by means of covalent functionalization of CNTs or noncovalent interactions with various functional molecules/polymers.<sup>[1]</sup> Although the latter method guarantees the retention of the  $\pi$ -conjugated system of CNTs while safeguarding their native properties, the weak interactions involved could give rise to nanocomposites that suffer from poor stability. Therefore, the covalent functionalization method represents the suitable alternative to enhance the stability of CNTs-based hybrids.

Among the non-destructive functionalization methods of CNTs networks, self-polymerization of dopamine (2-(3,4-dihydroxyphenyl)ethylamine) to generate polydopamine (PDA)<sup>[2]</sup> represents a very powerful approach to form a uniform polymeric coating onto almost all types of organic/inorganic surfaces, including CNTs.<sup>[3]</sup> The great potential offered by PDA coating becomes evident when certain aspects are taken into consideration. First, the great appeal of this functionalization method relies on its simplicity. As a matter of fact, only a dispersion of the material to be covered in a slightly alkaline aqueous solution of dopamine at room temperature is required to accomplish the covering process. In addition, the polymeric coating of PDA can serve as platform for the introduction of other surface functionalities. The strong adhesion properties of dopamine arise from the presence of catechol moieties that under oxidative conditions can generate o-quinone derivatives, which in addition to the self-polymerization process, can undergo further reaction with various functional groups, i.e. amines or thiols, by means of Michael addition or Schiff base reaction.<sup>[4]</sup> Furthermore, focusing on CNTs-based materials, PDA coating of pristine CNTs or the interaction of a preformed PDA layer with the surface of functionalized CNTs have been

[a] A. Mercadante, Dr. V. Campisciano, A. Morena, L. Valentino, Prof. M. Gruttadauria, Prof. F. Giacalone  
Department of Biological, Chemical and Pharmaceutical Sciences and Technologies (STEBICEF) and INSTM Udr – Palermo  
University of Palermo  
Viale delle Scienze, Ed. 17, 90128 Palermo, Italy  
E-mail: vincenzo.campisciano@unipa.it  
francesco.giacalone@unipa.it

[b] A. Morena, Prof. C. Aprile  
Unit of Nanomaterials Chemistry,  
Department of Chemistry, NISM  
University of Namur  
61 rue de Bruxelles, 5000 Namur, Belgium

[c] Dr. V. La Parola  
Institute for the Study of Nanostructured Materials (ISMN)  
(Italian) National Research Council (CNR)  
Via Ugo La Malfa 153, 90146 Palermo, Italy

Supporting information for this article is available on the WWW under  
<https://doi.org/10.1002/ejoc.202200497>

Part of the "DCO-SCI Prize and Medal Winners 2020/2021" Special Collection.

© 2022 The Authors. European Journal of Organic Chemistry published by Wiley-VCH GmbH. This is an open access article under the terms of the Creative Commons Attribution Non-Commercial NoDerivs License, which permits use and distribution in any medium, provided the original work is properly cited, the use is non-commercial and no modifications or adaptations are made.

proposed for a wide range of uses including sensing,<sup>[5]</sup> environmental applications,<sup>[6]</sup> membranes technology,<sup>[7]</sup> catalysis,<sup>[8]</sup> nanocomposites with enhanced properties,<sup>[9]</sup> wearable electronics,<sup>[10]</sup> biosensors,<sup>[11]</sup> and biomedical applications,<sup>[12]</sup> among others.

Given the great research interest aroused by CNTs-based composites, we believe that the direct introduction of catechol moieties, which can serve as anchoring points of further functionalities, onto the CNTs sidewalls could represent a valuable alternative to PDA coating, paving the way to further applications of such hybrid materials in other fields such as heterogeneous catalysis.<sup>[13]</sup> Georgakilas, Zbořil, Prato *et al.* proposed the functionalization of both single- (SWCNTs) and multiwalled carbon nanotubes (MWCNTs) with catechol groups via 1,3-dipolar cycloaddition using *N*-methylglycine and 3,4-dihydroxybenzaldehyde as solution to improve the processability of CNTs and facilitating the preparation of hybrid composites.<sup>[14]</sup> However, the adopted reaction conditions required long reaction time and a moderate degree of functionalization up to one functional group every 79 carbon atoms was reached. Since their seminal work, many efforts have been made to improve the functionalization efficiency of CNTs by means of the application of the 1,3-dipolar cycloaddition approach through both microwave mediated processes<sup>[15]</sup> and in the solid state,<sup>[16]</sup> achieving a higher functionalization degree of one functional group every 30 carbon atoms in the latter case.

Another effective and versatile approach for the covalent modification of CNTs consists in their coupling with preformed diazonium compounds<sup>[17]</sup> or generated *in situ* by action of isoamyl nitrite on aniline derivatives.<sup>[18]</sup> Herein, we chose to use 4-aminocatechol for the functionalization of MWCNTs by means of the generation of the corresponding diazonium salt formed through the reaction with isoamyl nitrite. The as-prepared MWCNTs-catechol hybrid showed a good dispersibility in water and other polar solvents such as methanol, ethanol, and *N,N*-dimethylformamide, proving the enhanced hydrophilicity upon functionalization. It is worth to note that in addition to the aforementioned reactions with amines and thiols with the reactive o-quinone derivatives, catechol can be exploited for its metal ion binding ability.<sup>[19]</sup> Therefore, the presence of catechol groups onto the surface of MWCNTs paves the way to further modification of the obtained material whether exploiting the dopamine-like chemistry of the catechol moieties or using their chelating ability for the formation of metal-based hybrid materials. In this work we have taken advantage of the nature of MWCNTs-catechol hybrid to deposit Pd(II) ions on its surface with the formation of catechol-Pd coordination complexes, which gave rise to Pd nanoparticles (NPs) after the treatment with NaBH<sub>4</sub> as reducing agent. The so-obtained MWCNTs-catechol-Pd material was used as recyclable catalyst in two C–C coupling reactions, namely Suzuki and Heck reactions.

## Results and Discussion

4-Nitrocatechol (1) was firstly quantitatively reduced to 4-aminocatechol (2) by means of catalytic hydrogenation on Pd/C.<sup>[20]</sup> Subsequently, the reaction of pristine MWCNTs with 2 in presence of isoamyl nitrite gave rise to **MWCNT-cat** material. **MWCNT-cat** was used as support for metal species through the immobilization of Pd(II) ions from an aqueous solution of Pd(NO<sub>3</sub>)<sub>2</sub>, affording **MWCNTs-cat Pd(II)**, followed by reduction with sodium borohydride to obtain the final **MWCNTs-cat Pd(0)** material (Scheme 1).

**MWCNT-cat** and **MWCNT-cat Pd(0)** were firstly characterized by means of thermogravimetric analysis/derivative thermogravimetry (TGA/DTG) under nitrogen atmosphere between 100 and 1000 °C. Both materials started to degrade above 140 °C. However, at high temperature, the analysis of the DTG profiles highlighted how the two materials exhibited a different behavior being the degradation of **MWCNT-cat** centered at 226 °C and more pronounced than a slower degradation rate of **MWCNT-cat Pd(0)** with a maximum slope of TG curve at 251 °C (Figure 1a). Degradation of **MWCNT-cat** and **MWCNT-cat Pd(0)** materials proceeded with no remarkable change in the slope of their thermogravimetric curves up to about 800 °C, temperature at which both materials started to drastically decompose due to the low stability at high temperature of the support material

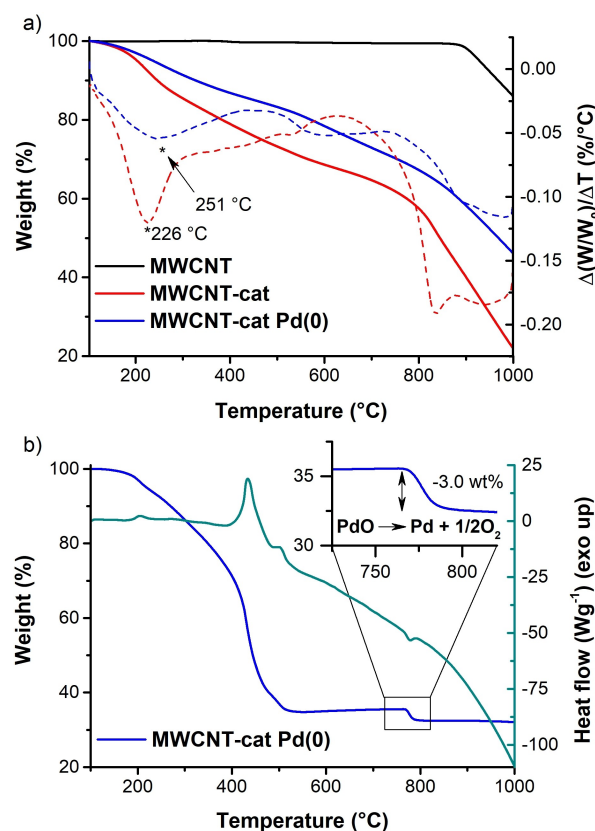
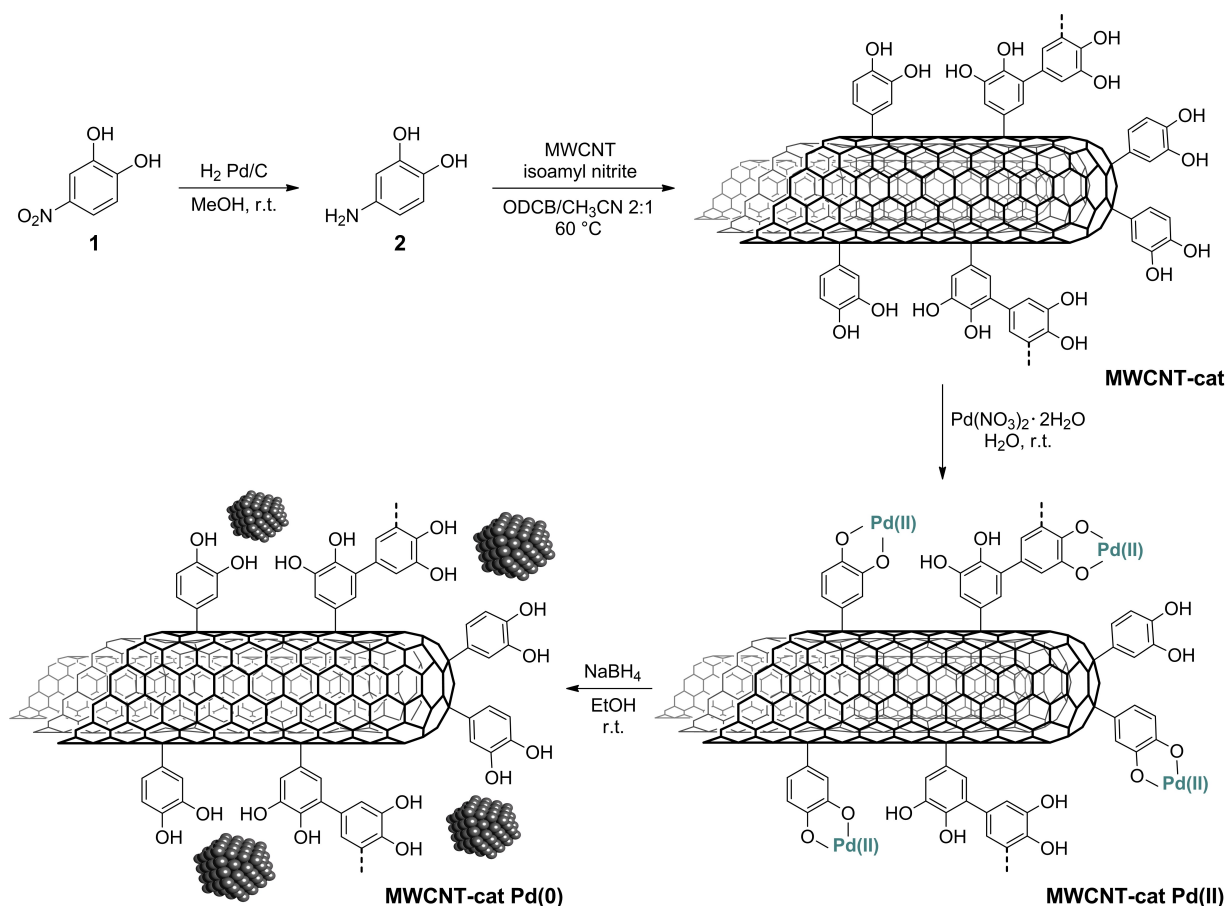


**Figure 1.** a) TGA (solid lines) and DTG (dotted lines) under N<sub>2</sub> of pristine MWCNT, MWCNT-cat and MWCNT-cat Pd(0), b) TGA/DSC under air flow of MWCNT-cat Pd(0).



**Scheme 1.** Preparation of **MWCNT-cat Pd(0)**. Please note that the chemical structures of **MWCNT-cat**, **MWCNT-cat Pd(II)** and **MWCNT-cat Pd(0)** are meant as simplified examples of the real branched structures.

(Figure 1a, black line). On the other hand, pristine MWCNT showed no weight loss up to 850 °C. This allowed to estimate the functionalization degree of **MWCNT-cat** corresponding to 35.3 wt%, which was calculated from the weight loss at 700 °C. This high loading can be explained if the formation of a multilayer is assumed during the functionalization of MWCNT, as was previously reported.<sup>[21]</sup> **MWCNT-cat Pd(0)** was also analyzed by means of TGA coupled with differential scanning calorimetry (DSC) under air atmosphere flow (Figure 1b). This technique was useful to provide first evidence of the presence of palladium species, which are oxidized to PdO during the heating. As a matter of fact, TGA profile of **MWCNT-cat Pd(0)** exhibited a small weight loss of 3 wt% between 760 and 800 °C that DSC associate to an endothermic process due to the decomposition of PdO, which is not stable over 800 °C,<sup>[22]</sup> to Pd(0) and molecular oxygen. This degradation step allowed to obtain a first estimation of the Pd content of **MWCNT-cat Pd(0)** corresponding to about 20 wt%. Furthermore, the Pd content of **MWCNT-cat Pd(0)** was determined by means of inductively coupled plasma optical emission spectroscopy (ICP-OES) analysis. The estimated metal loading of 20.3 wt% was in excellent agreement with the result obtained by TGA, highlighting the validity of the latter method for the estimation of Pd content.

X-ray photoelectron spectroscopy (XPS) analysis was used to determine the oxidation state of Pd species. The XPS spectrum of **MWCNT-cat Pd(II)** (Figure S1) displayed the presence of two peaks due to the typical spin-orbit splitting ( $\text{Pd}3d_{5/2}$  and  $\text{Pd}3d_{3/2}$ ) at the binding energy (BE) of 337.6 and 343.2 eV, respectively, corresponding to the Pd in its higher oxidation state. Therefore, the presence of oxidizable catechol moieties was not sufficient to reduce palladium species. A similar behavior was observed by Li, Zhang *et al.*<sup>[23]</sup> who used a catechol-functionalized microporous organic polymer as support for Pd NPs. The treatment with  $\text{NaBH}_4$  was thus necessary for the reduction of palladium(II) ions. XPS spectrum of **MWCNT-cat Pd(0)** confirmed the presence of reduced palladium with the appearance of a new couple of peaks centered at 336.1 and 341.5 eV attributed to the  $\text{Pd}3d_{5/2}$  and  $\text{Pd}3d_{3/2}$  components of Pd(0) (Figure 2). **MWCNT-cat Pd(0)** exhibited a palladium reduction degree of 68 %.

Both pristine MWCNT and **MWCNT-cat** and **MWCNT-cat Pd(0)** materials were analyzed by means of transmission electron microscopy (TEM) (Figure 3). Pristine MWCNT are arranged to form a set of bundles consisting of distinct long tubular structures (Figure 3a–b). Functionalization of pristine MWCNT with catechol moieties do not improve the dispersion of CNT, which are still grouped in large aggregates, probably



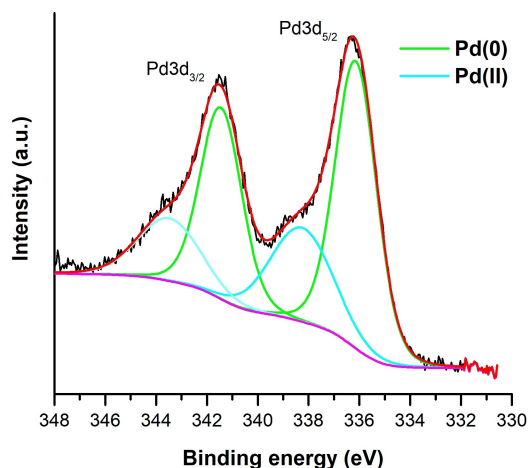


Figure 2. High-resolution XPS spectrum of Pd3d region of MWCNT-cat Pd(0).

due to the establishment of strong H-bond and  $\pi$ - $\pi$  interactions that could occur between the catechol functionalized carbonaceous skeletons of CNT in MWCNT-cat material (Figure 3c–d). The deposition of palladium species followed by their reduction with  $\text{NaBH}_4$  led to the formation of Pd nanoparticles (NPs) with a mean diameter of  $5.7 \pm 2.8$  nm ( $n=246$ ; see Figure S2 for average size distribution of Pd NPs) uniformly distributed over the whole surface of MWCNT-cat Pd(0), along with the presence of larger aggregates (Figure 3e–f).

Once characterized, MWCNT-cat Pd(0) was tested as catalyst in the Suzuki reaction between different arylboronic acids and aryl bromides in aqueous medium ( $\text{H}_2\text{O}/\text{EtOH}$  1:1) using  $\text{K}_2\text{CO}_3$  as base and a catalytic loading of 0.2 mol % at  $50^\circ\text{C}$  for 4 h (Table 1). The coupling of phenylboronic acid with aryl

bromides (Table 1, entries 1–9) afforded the corresponding biphenyl derivatives with good to excellent yields. Aryl bromides with electron-withdrawing groups resulted more reactive (Table 1, entries 1–5) than electron-donating substituted ones (Table 1, entries 6–9). The same trend was followed when 4-methoxyphenylboronic acid was employed (Table 1, entries 10–13). A high yield was obtained from the reaction between 4-formylphenylboronic acid and 4-bromobenzaldehyde (Table 1, entries 14), whereas the use of 5-formyl-2-thienylboronic acid gave rise to a moderate yield of 25% (Table 1, entries 15).

The reaction between phenylboronic acid and 4-bromobenzaldehyde was chosen as model reaction to test the recyclability of MWCNT-cat Pd(0). Unfortunately, MWCNT-cat Pd(0) displayed a marked drop in its catalytic activity already after the first run making this catalyst not recyclable in the adopted reaction conditions (Table S1).

To shed light on the reason for the drop in catalytic activity of MWCNT-cat Pd(0), further investigations were carried out on the spent catalyst. XPS measurements displayed a lower reduction degree (57%) of Pd after the recycling experiments than fresh catalyst (Figure S3). A possible explanation of this finding was provided by TEM images of the spent catalyst after 5 cycles (Figure S4). Pd NPs with slightly bigger diameters ( $6.9 \pm 2.5$  nm;  $n=159$ , average size distribution of Pd NPs shown in Figure S5) than those of the fresh catalyst ( $5.7 \pm 2.8$  nm) were observed. Moreover, reused MWCNT-cat Pd(0) showed a lower number of Pd NPs and, unlike fresh catalyst, almost no bigger aggregates were detected. The absence of large aggregates could explain the reason of the apparent oxidation of Pd after the recycling runs. In fact, if only small NPs are present on the surface of the spent catalyst, the percentage of exposed metal surface susceptible to oxidation is higher, which means a lower

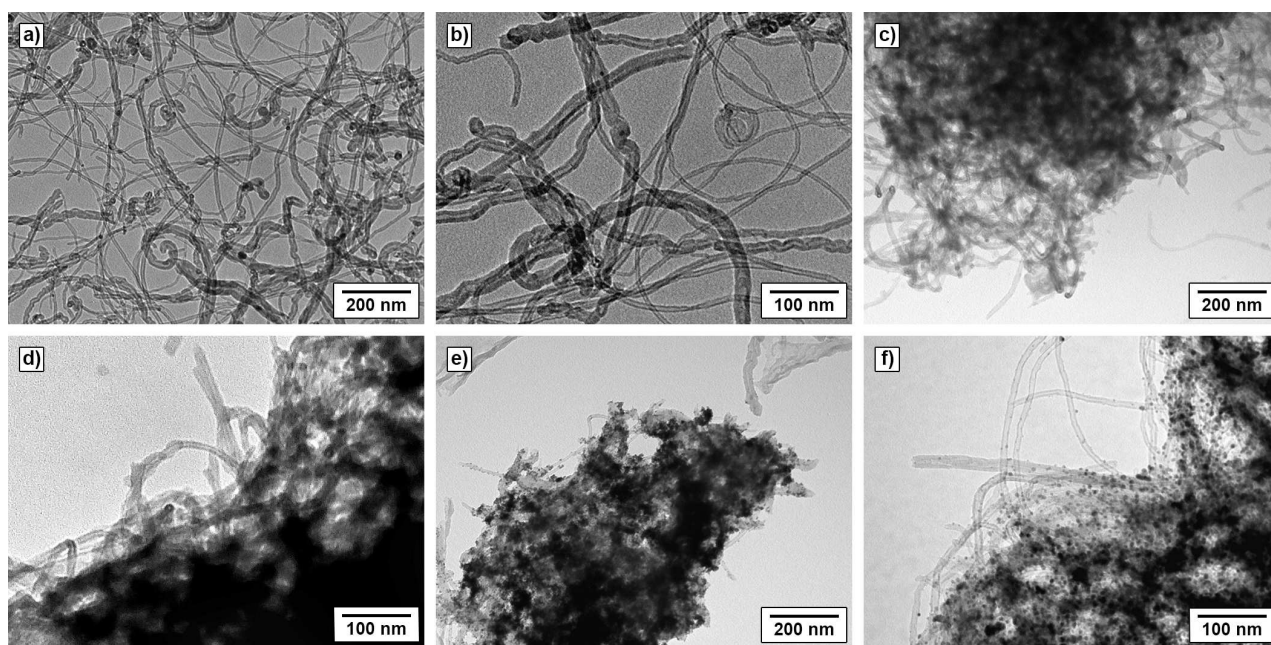
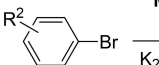
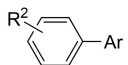
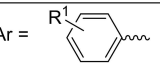
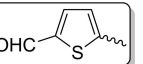
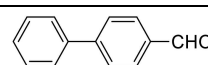
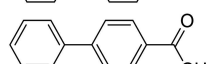
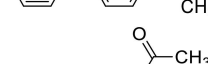
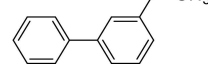
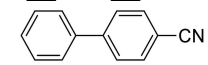
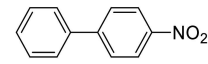
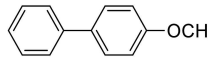
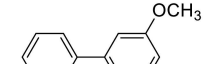
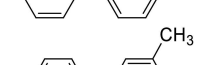
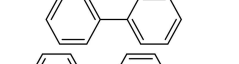
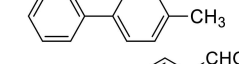
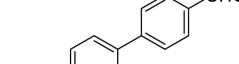
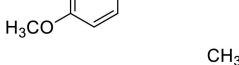
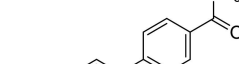
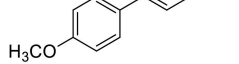


Figure 3. TEM images of a–b) pristine MWCNT, c–d) MWCNT-cat, and e–f) MWCNT-cat Pd(0).

Table 1. Suzuki reactions catalyzed by MWCNT-cat Pd(0).<sup>[a]</sup>

<div>Ar-B(OH)<sub>2</sub> +  <math>\xrightarrow[\text{K}_2\text{CO}_3, \text{H}_2\text{O/EtOH 1:1}, 50^\circ\text{C}, 4\text{ h}]{\text{MWCNT-cat Pd(0) 0.2 mol\%}}</math> </div>				
<div>Ar =  </div>				
Entry	R <sup>1</sup>	R <sup>2</sup>	Product	Yield <sup>[b]</sup> [%]
1	4-H	4-CHO		99
2	4-H	4-COCH <sub>3</sub>		99
3	4-H	3-COCH <sub>3</sub>		78
4	4-H	4-CN		96
5	4-H	4-NO <sub>2</sub>		73
6	4-H	4-OCH <sub>3</sub>		54
7	4-H	3-OCH <sub>3</sub>		48
8	4-H	3-CH <sub>3</sub>		69
9	4-H	4-CH <sub>3</sub>		69
10	4-OCH <sub>3</sub>	4-CHO		93
11	4-OCH <sub>3</sub>	4-COCH <sub>3</sub>		98
12	4-OCH <sub>3</sub>	4-OCH <sub>3</sub>		78
13	4-OCH <sub>3</sub>	3-CH <sub>3</sub>		70
14	4-CHO	4-CHO		86
15	–	4-CHO		25

[a] Reaction conditions: aryl bromide (0.5 mmol), phenylboronic acid (0.55 mmol), K<sub>2</sub>CO<sub>3</sub> (0.6 mmol), EtOH/H<sub>2</sub>O (1 : 1, 1 mL), catalyst (0.5 mg; 0.2 mol % - determined by ICP-OES). [b] Isolated yield.

reduction degree. Since the number of Pd NPs was remarkably lower in the reused catalyst, it was assumed that metal leaching could occur. To demonstrate this, three parallel reactions between 4-bromoanisole and phenylboronic acid in the presence of **MWCNT-cat Pd(0)** at 0.4 mol % at 50 °C were carried out. The first one was stopped after 30 minutes and the reaction mixture was analyzed by <sup>1</sup>H NMR giving rise to a conversion degree of (58%). The second one was filtered while still hot (hot filtration) after 30 minutes and the filtrate was allowed to react for further 3 hours and 30 minutes giving rise to full conversion into the corresponding biaryl compound. The third one, was filtered after 30 minutes of reaction plus an additional time in order to reach room temperature (cold filtration) and the filtrate was allowed to react for further 3 hours and 30 minutes leading to a 92% conversion. The reference reaction carried out for 4 h without the removal of catalyst furnished the product in full conversion. The results of hot and cold filtration test demonstrated the presence of soluble active Pd species that were not recaptured by the catalyst after the cooling down of the reaction mixture leading to metal leaching in solution, which can explain both the loss of catalytic activity during the recycling runs and the lower number of Pd NPs in the spent catalyst observed in the TEM images.

We decided to test **MWCNT-cat Pd(0)** in another C–C coupling reaction, namely Heck reaction between methyl acrylate/styrene and a series of aryl iodides (Table 2 and Table 3).

**MWCNT-cat Pd(0)** proved to be an active catalyst for the Heck reaction allowing to reach very high or quantitative yields of all the substrates investigated with a reaction time of 3 h. The adopted reaction conditions involved the use of triethylamine as base, dimethylformamide as solvent and a catalyst loading of 0.2 mol % at 100 °C. When styrene was used, high selectivity (>86%) towards *trans*- vs. *gem*-alkene was reached (Table 3).

Moreover, a less reactive aryl bromide, namely 4-bromobenzaldehyde, was satisfactorily converted (85%) into the corresponding coupling product using the same catalytic loading of 0.2 mol % in a longer reaction time of 5 h (Table 3, entry 8).

Further studies were carried out to assess if **MWCNT-cat Pd(0)** could be recycled in the selected conditions. The coupling between methyl acrylate and 4-iodoanisole was chosen as model reaction to assess the recyclability of **MWCNT-cat Pd(0)** (Figure 4).

Unlike the case of the Suzuki reaction, **MWCNT-cat Pd(0)** proved to be a recoverable and reusable catalyst for the Heck reaction. As a matter of fact, the recovery of **MWCNT-cat Pd(0)** from the reaction mixture by simple centrifugation allowed it to be reused for 5 runs at 0.2 mol % without loss of its catalytic activity affording quantitative yields (Figure 4, cycles 1–5). In light of the good results obtained, the recycled catalyst used for five cycles was employed in two additional runs with a lower loading of 0.04 mol %. Once again, quantitative yields were obtained (Figure 4, cycles 6–7). Finally, the catalytic loading was further reduced down to 0.02 mol % for the 8<sup>th</sup> and 9<sup>th</sup> cycles

**Table 2.** Heck reactions between methyl acrylate and aryl iodides catalyzed by MWCNT-cat Pd(0).<sup>[a]</sup>

Entry	R <sup>1</sup>	Product	Yield <sup>[b]</sup> [%]
1	4-CHO		91
2	4-COCH <sub>3</sub>		99
3	4-NO <sub>2</sub>		90
4	4-OCH <sub>3</sub>		99
5	3-OCH <sub>3</sub>		98
6	4-CH <sub>3</sub>		99
7	2-CH <sub>3</sub>		99
8	H		97

[a] Reaction conditions: aryl iodide (0.5 mmol), methyl acrylate (0.75 mmol), triethylamine (1 mmol), DMF (1 mL), catalyst (0.5 mg; 0.2 mol % - determined by ICP-OES). [b] Isolated yield.

affording 97 and 99 % yield, respectively (Figure 4, cycles 8–9), and reaching a total turnover number (TON) of 17,500.

The spent catalyst (after the 5<sup>th</sup> cycle) used in the recycling experiments was subjected to XPS measurements showing a slightly higher reduction degree of the palladium species with respect to the fresh catalyst (74 % vs. 68 %) (Figure 5).

Further investigations by means of TEM analysis on the used catalyst (after the 5<sup>th</sup> cycle) showed that agglomeration phenomena of the Pd NPs in some extent took place during reuse (Figure 6), and the mean diameter and the polydispersity increased up to  $19.3 \pm 11.7$  nm ( $n = 124$ ; see Figure S6 for average size distribution of Pd NPs). A similar behavior was also reported in the case of a Pd/CNTs-PDA hybrid material in which the dimension of Pd NPs increased after recycling causing a partial reduction of catalytic activity.<sup>[80]</sup> However, in this case, despite the agglomeration process of Pd NPs, MWCNT-cat Pd(0) showed no loss of catalytic activity.

**Table 3.** Heck reactions between styrene and aryl halides catalyzed by MWCNT-cat Pd(0).<sup>[a]</sup>

Entry	R <sup>1</sup>	X	Product	Sel. <sup>[b]</sup> /Yield <sup>[c]</sup> [%]
1	4-CHO	I		96/98
2	4-COCH <sub>3</sub>	I		97/90
3	4-NO <sub>2</sub>	I		94/91
4	4-OCH <sub>3</sub>	I		86/97
5	3-OCH <sub>3</sub>	I		88/85
6	4-CH <sub>3</sub>	I		97/97
7	2-CH <sub>3</sub>	I		92/98
8 <sup>[d]</sup>	4-CHO	Br		94/85

[a] Reaction conditions: aryl halide (0.5 mmol), styrene (0.75 mmol), triethylamine (1 mmol), DMF (1 mL), catalyst (0.5 mg; 0.2 mol % - determined by ICP-OES). [b] Selectivity (indicated in italics) towards *trans*-alkene, determined by <sup>1</sup>H NMR. [c] Isolated yield (indicated in bold) of *gem*- and *trans*-alkene. [d] 5 h.

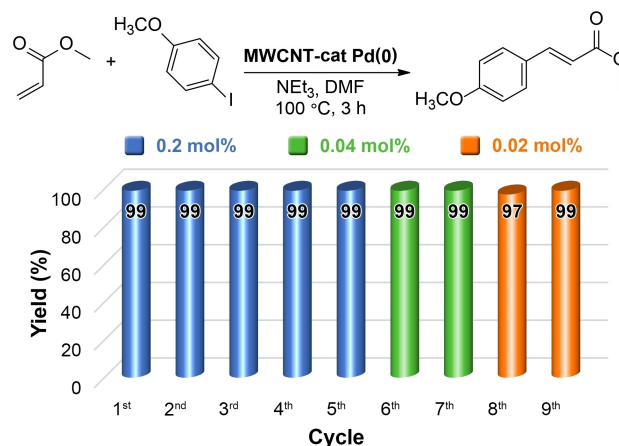


**Figure 4.** Recycling experiments in the Heck reaction between methyl acrylate and 4-iodoanisole. Reaction conditions: 4-iodoanisole (2.5 mmol), methyl acrylate (3.75 mmol), triethylamine (5 mmol), DMF (2.5 mL), catalyst (0.2–0.02 mol %). (Blue bars) 2.5 mg of catalyst were used. (Green bars) 0.5 mg of catalyst were used. (Orange bars) 0.25 mg of catalyst were used.

The increased dimension of Pd NPs could also explain the reason of higher reduction degree detected by XPS analysis. Since XPS is a surface-sensitive technique and Pd NPs are subjected to surface partial oxidation, for fixed amount of palladium, small NPs offer a wider total surface area than bigger



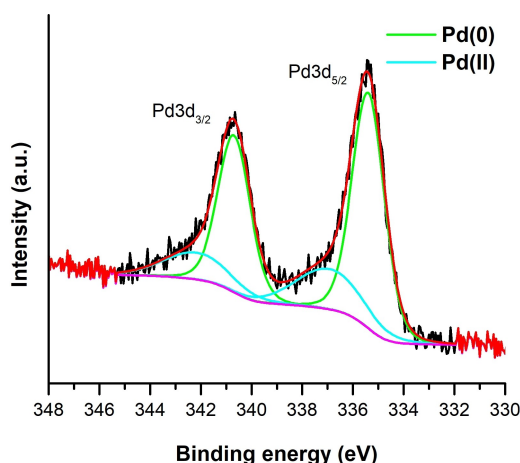


**Figure 5.** High-resolution XPS spectrum of Pd3d region of **MWCNT-cat Pd(0)** after the 5<sup>th</sup> cycle of the Heck reaction.

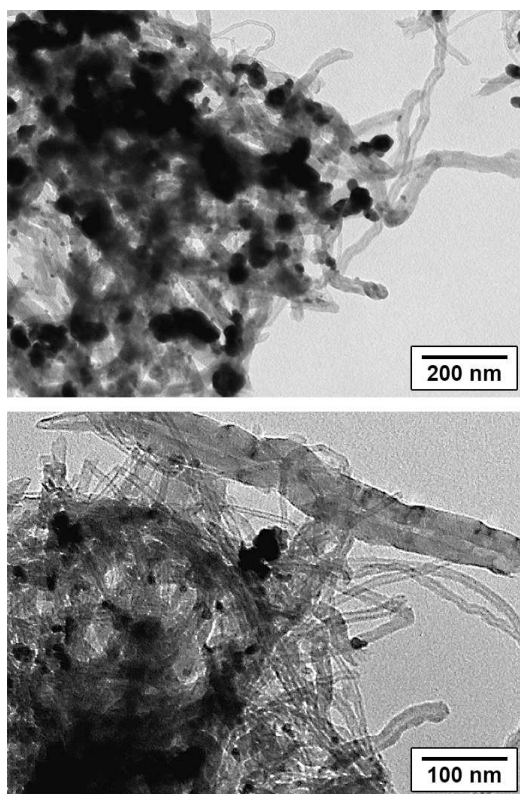


**Figure 6.** TEM images of **MWCNT-cat Pd(0)** after the 5<sup>th</sup> cycle of the Heck reaction.

NPs. This means that the higher Pd(0)/Pd(II) ratio in the spent catalyst could be due to the agglomeration process of NPs.

Finally, although comparing different catalytic systems is always a difficult task due to the different reaction conditions and/or catalytic loading adopted, the catalytic system presented by Run, Sun *et al.*,<sup>[80]</sup> consisting of the decoration of polydopamine-coated MWCNTs with Pd NPs (Pd/CNTs-PDA) by means of a one-pot approach, could represent an interesting compar-

ison with the here presented **MWCNT-cat Pd(0)** catalyst. Pd/CNTs-PDA was used with a catalytic loading of 0.15 mol% in the Heck reaction between different aryl iodides and methyl acrylate showing results comparable with those here reported. The main difference lies in the recycling ability of the two catalytic systems. In fact, if on the one hand Pd/CNTs-PDA was reused for five cycles with a slight loss of catalytic activity, on the other hand **MWCNT-cat Pd(0)** catalyst retained its activity during nine cycles even after reducing its catalytic loading down to 0.02 mol%. This proves how the direct introduction of catechol moieties onto the CNTs sidewalls could represent a valuable alternative to PDA coating.

## Conclusion

In conclusion, the generation of the diazonium salt formed through the reaction between 4-aminocatechol and isoamyl nitrite was exploited to functionalize MWCNT. A good degree of functionalization was reached and the modified MWCNT were used as support for Pd NPs. The material obtained was fully characterized and the hybrid material **MWCNT-cat Pd(0)** was tested as catalyst in two C–C coupling reactions, namely Suzuki and Heck reactions. Despite good results reached in the Suzuki reaction between phenylboronic acid and different aryl bromides, the recycling experiments of **MWCNT-cat Pd(0)** showed a fast loss of catalytic activity. In contrast, in the case of the Heck reaction, both the catalytic tests between methyl acrylate/styrene and a series of aryl iodides and the recycling experiments gave excellent results. It was possible to use **MWCNT-cat Pd(0)** catalyst up to nine cycles without loss of catalytic activity decreasing the catalytic loading down to 0.02 mol% and achieving a cumulative TON of 17,500. XPS and TEM analyses showed that the spent catalyst exhibited a slightly higher reduction degree of Pd and an increase in the mean size of Pd NPs. These findings open the way to new possible application for CNF-catechol hybrids further modified with other metal nanoparticles or organometallic complexes to develop highly active and recyclable catalysts.

## Experimental Section

Chemicals and solvents were purchased from commercial suppliers (TCI, Fluorochem, Merck, VWR) and used as received without further purification. Thermogravimetric analyses (TGA) were performed under nitrogen or air flow from 100 to 1000 °C with a heating rate of 10 °C·min<sup>-1</sup> with a Mettler Toledo TGA/DSC STAR System. All samples were maintained at 100 °C for 30 minutes to remove the adsorbed water. Inductively coupled plasma optical emission spectroscopy (ICP-OES) was performed in an Optima 8000 ICP-OES Spectrometer. The X-ray photoelectron spectroscopy (XPS) analyses were performed with a VG Microtech ESCA 3000 Multilab, equipped with a dual Mg/Al anode. As excitation source was used the Al K $\alpha$  radiation (1486.6 eV). The sample powders were mounted on a double-sided adhesive tape. The pressure in the analysis chamber was in the range of 10<sup>-8</sup> Torr during data collection. The constant charging of the samples was removed by referencing all the energies to the C 1s binding energy set at 285.1 eV. Analyses of the peaks were performed with the CasaXPS software.<sup>[24]</sup> Transmission



electron microscopy (TEM) images were recorded on a Philips TECNAI 10 microscope at 80 kV.  $^1\text{H}$  and  $^{13}\text{C}$  NMR spectra were recorded on a Bruker 400 MHz spectrometer using  $\text{CDCl}_3$  as solvent. Mass spectra were obtained using a GC-MS apparatus (Agilent technologies 7000 C GC/MS Triple Quad – 7890B GC System) at 70 eV ionization voltage.

**Synthesis of 4-aminocatechol (2).** 4-Aminocatechol (2) was synthesized following a previously reported procedure.<sup>[20]</sup> Briefly, 4-nitrocatechol (1, 1.55 g, 10.0 mmol) was dissolved in MeOH (65 mL), 10 wt% Pd/C (100 mg) was added and the reaction mixture was stirred at room temperature under a hydrogen atmosphere for 2.5 h. After the reaction was completed, the reaction mixture was filtered under vacuum on Celite using MeOH. The filtrate was concentrated under reduced pressure to obtain the crude product, which was used without further purification, in quantitative yield as a dark red powder.

**Preparation of MWCNT-cat.** In a two-necked round bottom flask, 100 mg of MWCNT were dispersed in 50 mL of 1,2-dichlorobenzene (ODCB) by means of sonication (15 minutes). To this suspension, a solution of 4-aminocatechol (2, 500 mg, 4.0 mmol) in 25 mL of acetonitrile was added. The reaction mixture was placed under inert atmosphere (Ar) and argon was bubbled in the solution for 10 minutes at room temperature to remove the dissolved oxygen before adding isoamyl nitrite (6.0 mmol) and raising the temperature up to 60 °C. The reaction mixture was reacted overnight under stirring at this temperature. The suspension was cooled to room temperature, diluted with 30 mL of dimethylformamide, filtered under vacuum on a PTFE membrane (0.45  $\mu\text{m}$ ), and washed extensively with DMF, methanol and diethyl ether. **MWCNT-cat** was obtained as a dark powder (176 mg).

**Preparation of MWCNT-cat Pd(0).** In a round bottom flask,  $\text{Pd}(\text{NO}_3)_2 \cdot 2\text{H}_2\text{O}$  (90 mg, 0.34 mmol) was solubilized in 25 mL of water. To this solution, 140 mg of **MWCNT-cat** were added. The reaction mixture was sonicated (5 minutes) and then placed under stirring at room temperature for 20 h. The reaction mixture was filtered under vacuum on a PTFE membrane (0.45  $\mu\text{m}$ ), washed with water, methanol, diethyl ether, and dried under reduced pressure at 60 °C. **MWCNT-cat Pd(II)** was resuspended in ethanol (10 mL) and to this suspension, a solution of  $\text{NaBH}_4$  (20 mg, 0.54 mmol) in anhydrous ethanol (2 mL) was added dropwise. The reaction mixture was stirred at room temperature for 6 h, then filtered under vacuum (PTFE membrane, 0.45  $\mu\text{m}$ ), washed with water, ethanol, and diethyl ether, and dried overnight under reduced pressure at 60 °C. **MWCNT-cat Pd(0)** was obtained as a dark powder (168 mg).

**General procedure for the Suzuki reactions.** In a 5 mL glass vial with screw cap, **MWCNT-cat Pd(0)** (0.5 mg, 0.2 mol%), aryl bromide (0.5 mmol), phenylboronic acid (0.55 mmol),  $\text{K}_2\text{CO}_3$  (0.6 mmol), and EtOH/ $\text{H}_2\text{O}$  (1:1, 1 mL) were added. The reaction mixture was stirred at 50 °C for 4 h, then allowed to cool down to room temperature and extracted with dichloromethane (3 times). The combined organic layers were dried over  $\text{MgSO}_4$  and evaporated under reduced pressure to obtain the crude product. The product was purified by column chromatography (hexane/ethyl acetate as eluent).

**Recycling procedure of MWCNT-cat Pd(0) in the Suzuki reaction.** In a 12 mL glass vial with screw cap, **MWCNT-cat Pd(0)** (5.0 mg, 0.2 mol%), 4-bromobenzaldehyde (925 mg, 5.0 mmol), phenylboronic acid (665 mg, 5.5 mmol),  $\text{K}_2\text{CO}_3$  (829 mg, 6.0 mmol), and EtOH/ $\text{H}_2\text{O}$  (1:1, 5 mL) were added. The reaction mixture was stirred at 50 °C for 4 h, then allowed to cool down to room temperature and centrifuged removing the supernatant. The residue was washed by sonication and centrifugation with dichloromethane, methanol and

diethyl ether. The recovered catalyst was dried in an oven at 60 °C overnight before its use in the next cycle. All the combined supernatants were evaporated at reduced pressure and the residue was taken up with dichloromethane and extracted (3 times) with the same solvent. The combined organic layers were dried over  $\text{MgSO}_4$  and evaporated under reduced pressure to obtain the crude product. The product was purified by column chromatography (hexane/ethyl acetate as eluent).

**General procedure for the hot and cold filtration test.** In two 5 mL glass vial with screw cap, **MWCNT-cat Pd(0)** (1.0 mg, 0.4 mol%), 4-bromoanisole (0.5 mmol), phenylboronic acid (0.55 mmol),  $\text{K}_2\text{CO}_3$  (0.6 mmol), and EtOH/ $\text{H}_2\text{O}$  (1:1, 1 mL) were added. The mixtures were stirred at 50 °C for 30 minutes. In the hot filtration test, the reaction mixture was filtered while still hot and the filtrate was allowed to react for additional 3 h and 30 minutes. In the cold filtration test, the reaction mixture was allowed reach room temperature and filtered, the filtrate was allowed to react for additional 3 h and 30 minutes. The filtrates were then allowed to cool down to room temperature and extracted with dichloromethane (3 times). The combined organic layers were dried over  $\text{MgSO}_4$  and evaporated under reduced pressure to obtain the crude product. The conversions were determined by  $^1\text{H}$  NMR analysis.

**General procedure for the Heck reactions.** In a 5 mL glass vial with screw cap, **MWCNT-cat Pd(0)** (0.5 mg, 0.2 mol%), aryl iodide (0.5 mmol), methyl acrylate (0.75 mmol), triethylamine (1 mmol), and DMF (1 mL) were added. The reaction mixture was stirred at 100 °C for 3 h, then allowed to cool down to room temperature and extracted with diethyl ether (3 times). The combined organic layers were dried over  $\text{MgSO}_4$  and evaporated under reduced pressure to obtain the crude product. The product was purified by column chromatography (hexane/ethyl acetate as eluent).

**Recycling procedure of MWCNT-cat Pd(0) in the Heck reaction.** In a 5 mL glass vial with screw cap, **MWCNT-cat Pd(0)** (2.5 mg, 0.2 mol%), 4-iodoanisole (596 mg, 2.5 mmol), methyl acrylate (337  $\mu\text{L}$ , 3.75 mmol), triethylamine (708  $\mu\text{L}$ , 5 mmol), and DMF (2.5 mL) were added. The reaction mixture was stirred at 100 °C for 3 h, then allowed to cool down to room temperature and centrifuged removing the supernatant. The residue was washed by sonication and centrifugation with ethyl acetate, methanol and diethyl ether. The recovered catalyst was dried in an oven at 60 °C overnight before its use in the next cycle. All the combined supernatants were evaporated at reduced pressure and the residue was taken up with diethyl ether and extracted (3 times) with the same solvent. The combined organic layers were dried over  $\text{MgSO}_4$  and evaporated under reduced pressure to obtain the crude product. The product was purified by column chromatography (hexane/ethyl acetate as eluent).

## Acknowledgements

*The authors gratefully acknowledge the University of Palermo and the Italian Ministry of Education, University and Research (MIUR) for financial support through PRIN 2017 (projects no. 2017W8KNZW and 2017YJMPZN). Open Access funding provided by Università degli Studi di Palermo within the CRUI-CARE Agreement.*

## Conflict of Interest

The authors declare no conflict of interest.

## Data Availability Statement

The data that support the findings of this study are available in the supplementary material of this article.

**Keywords:** Carbon nanotubes · C–C coupling reactions · Suzuki and Heck reactions · Palladium nanoparticles · Heterogeneous catalysis

- [1] a) K. Balasubramanian, M. Burghard, *Small* **2005**, *1*, 180–192; b) S. Banerjee, T. Hemraj-Benny, S. S. Wong, *Adv. Mater.* **2005**, *17*, 17–29; c) P. Singh, S. Campidelli, S. Giordani, D. Bonifazi, A. Bianco, M. Prato, *Chem. Soc. Rev.* **2009**, *38*, 2214–2230; d) D. Tasis, N. Tagmatarchis, A. Bianco, M. Prato, *Chem. Rev.* **2006**, *106*, 1105–1136; e) D. Tuncel, *Nanoscale* **2011**, *3*, 3545–3554; f) Z. Syrgiannis, A. Bonasera, E. Tenori, V. La Parola, C. Hadad, M. Gruttadauria, F. Giacalone, M. Prato, *Nanoscale* **2015**, *7*, 6007–6013; g) Z. Syrgiannis, V. La Parola, C. Hadad, M. Lucio, E. Vázquez, F. Giacalone, M. Prato, *Angew. Chem. Int. Ed.* **2013**, *52*, 6480–6483; *Angew. Chem.* **2013**, *125*, 6608–6611.
- [2] E. Herlinger, R. F. Jameson, W. Linert, *J. Chem. Soc. Perkin Trans. 2* **1995**, 259–263.
- [3] a) H. Lee, S. M. Dellatore, W. M. Miller, P. B. Messersmith, *Science* **2007**, *318*, 426–430; b) B. Fei, B. Qian, Z. Yang, R. Wang, W. C. Liu, C. L. Mak, J. H. Xin, *Carbon* **2008**, *46*, 1795–1797.
- [4] a) J. Liebscher, *Eur. J. Org. Chem.* **2019**, 2019, 4976–4994; b) M. J. LaVoie, B. L. Ostaszewski, A. Weihofen, M. G. Schlossmacher, D. J. Selkoe, *Nat. Med.* **2005**, *11*, 1214–1221; c) J. Yang, M. A. Cohen Stuart, M. Kamperman, *Chem. Soc. Rev.* **2014**, *43*, 8271–8298; d) J. Wu, L. Zhang, Y. Wang, Y. Long, H. Gao, X. Zhang, N. Zhao, Y. Cai, J. Xu, *Langmuir* **2011**, *27*, 13684–13691.
- [5] a) K. Manibalan, S. Han, Y. Zheng, H. Li, J.-M. Lin, *ACS Sens.* **2019**, *4*, 2450–2457; b) S. Chen, J. Xu, M. Shi, Y. Yu, Q. Xu, X. Duan, Y. Gao, L. Lu, *Appl. Surf. Sci.* **2021**, *570*, 151149; c) Z. Weng, R. Guan, F. Zou, P. Zhou, Y. Liao, Z. Su, L. Huang, F. Liu, *Carbon* **2020**, *170*, 403–413; d) S. Reddy, Q. Xiao, H. Liu, C. Li, S. Chen, C. Wang, K. Chiu, N. Chen, Y. Tu, S. Ramakrishna, L. He, *ACS Appl. Mater. Interfaces* **2019**, *11*, 18254–18267; e) A. R. Jalalvand, M. M. Zangeneh, F. Jalili, S. Soleimani, J. M. Díaz-Cruz, *Chem. Phys. Lipids* **2020**, *229*, 104895; f) M. Sabeti, A. A. Ensafi, K. Z. Mousaabadi, B. Rezaei, *IEEE Sens. J.* **2021**, *21*, 19714–19721; g) V. Mani, T. S. T. Balamurugan, S.-T. Huang, *Int. J. Mol. Sci.* **2020**, *21*, 2853; h) C. Zhang, S. Song, Q. Li, J. Wang, Z. Liu, S. Zhang, Y. Zhang, *J. Mater. Chem. C* **2021**, *9*, 15337–15345; i) J. Qian, Y. Yi, D. Zhang, G. Zhu, *Microchim. Acta* **2019**, *186*, 358; j) X. Zhang, J. Zheng, *Microchim. Acta* **2020**, *187*, 89; k) F. Chang, H. Wang, S. He, Y. Gu, W. Zhu, T. Li, R. Ma, *RSC Adv.* **2021**, *11*, 31950–31958.
- [6] a) X. Zhang, Q. Huang, M. Liu, J. Tian, G. Zeng, Z. Li, K. Wang, Q. Zhang, Q. Wan, F. Deng, Y. Wei, *Appl. Surf. Sci.* **2015**, *343*, 19–27; b) W. Zhan, L. Gao, X. Fu, S. H. Siyal, G. Sui, X. Yang, *Appl. Surf. Sci.* **2019**, *467*–468, 1122–1133; c) H. Wang, E. Wang, Z. Liu, D. Gao, R. Yuan, L. Sun, Y. Zhu, *J. Mater. Chem. A* **2015**, *3*, 266–273; d) M. R. Islam, M. Ferdous, M. I. Sujon, X. Mao, H. Zeng, M. S. Azam, *J. Colloid Interface Sci.* **2020**, *562*, 52–62; e) S. Zhao, Y. Zhan, X. Wan, S. He, X. Yang, J. Hu, G. Zhang, *J. Mol. Liq.* **2020**, *319*, 114289; f) S. S. Ghasemi, M. Hadavifar, B. Maleki, E. Mohammadnia, *J. Water Proc. Eng.* **2019**, *32*, 100965; g) S. Zhou, J. Zhang, Z. Yang, X. Zhang, *Langmuir* **2021**, *37*, 4523–4531.
- [7] a) F. Soyekwo, C. Liu, H. Wen, Y. Hu, *Chem. Eng. J.* **2020**, *380*, 122560; b) Y. Lu, Z. Wang, W. Fang, Y. Zhu, Y. Zhang, J. Jin, *Ind. Eng. Chem. Res.* **2020**, *59*, 22533–22540; c) Y. Gong, S. Gao, Y. Tian, Y. Zhu, W. Fang, Z. Wang, J. Jin, *J. Membr. Sci.* **2020**, *600*, 117874; d) F. Soyekwo, Q. Zhang, Y. Qu, Z. Lin, X. Wu, A. Zhu, Q. Liu, *AIChE J.* **2019**, *65*, 755–765; e) Y. Zhu, W. Xie, S. Gao, F. Zhang, W. Zhang, Z. Liu, J. Jin, *Small* **2016**, *12*, 5034–5041; f) L. Deng, Q. Wang, X. An, Z. Li, Y. Hu, *Desalination* **2020**, *479*, 114311; g) Y. Wang, Z. Zhang, T. Li, P. Ma, H. Zhang, M. Chen, M. Du, W. Dong, *ACS Appl. Mater. Interfaces* **2019**, *11*, 44886–44893; h) J. Zuo, Z. Liu, C. Zhou, Y. Zhou, X. Wen, S. Xu, J. Cheng, P. Pi, *J. Hazard. Mater.* **2021**, *403*, 123620; i) X. Zhao, L. Cheng, R. Wang, N. Jia, L. Liu, C. Gao, *J. Membr. Sci.* **2019**, *589*, 117257; j) J. Lu, Y. Qin, Y. Wu, M. Meng, Z. Dong, C. Yu, Y. Yan, C. Li, F. K. Nyarko, *J. Membr. Sci.* **2020**, *601*, 117917; k) X. Huang, S. Zhang, W. Xiao, J. Luo, B. Li, L. Wang, H. Xue, J. Gao, *J. Membr. Sci.* **2020**, *614*, 118500; l) S. Zarghami, T. Mohammadi, M. Sadrzadeh, B. Van der Bruggen, *Sci. Total Environ.* **2020**, *711*, 134951.
- [8] a) H. Huang, Z. He, X. Lin, W. Ruan, Y. Liu, Z. Yang, *Appl. Catal. A* **2015**, *490*, 65–70; b) K. Qu, Y. Zheng, Y. Jiao, X. Zhang, S. Dai, S.-Z. Qiao, *Adv. Energy Mater.* **2017**, *7*, 1602068; c) C. Wang, W. Gong, X. Lu, Y. Xiang, P. Ji, *ACS Omega* **2019**, *4*, 16808–16815; d) W. Ye, H. Hu, H. Zhang, F. Zhou, W. Liu, *Appl. Surf. Sci.* **2010**, *256*, 6723–6728; e) J. Sun, S. Wang, Y. Wang, H. Li, H. Zhou, B. Chen, X. Zhang, H. Chen, K. Qu, J. Zhao, *Catalysts* **2019**, *9*, 159; f) S. Tian, P. Yan, F. Li, X. Zhang, D. Su, W. Qi, *ChemCatChem* **2019**, *11*, 2073–2078; g) R. Sun, F. Ren, D. Wang, Y. Yao, Z. Fei, H. Wang, Z. Liu, R. Xing, Y. Du, *Colloids Surf. Physicochem. Eng. Aspects* **2019**, *578*, 123566; h) E. E. Arthur, F. Li, F. W. Y. Momade, H. Kim, *Energy* **2014**, *76*, 822–829; i) H. Yang, Q. Zhang, H. Zou, Z. Song, S. Li, J. Jin, J. Ma, *Int. J. Hydrogen Energy* **2017**, *42*, 13209–13216; j) Y. Gao, L. Wang, G. Li, Z. Xiao, Q. Wang, X. Zhang, *Int. J. Hydrogen Energy* **2018**, *43*, 7893–7902; k) S. Asmat, A. H. Anwer, Q. Husain, *Int. J. Biol. Macromol.* **2019**, *140*, 484–495; l) X.-C. Liu, G.-C. Wang, R.-P. Liang, L. Shi, J.-D. Qiu, *J. Mater. Chem. A* **2013**, *1*, 3945–3953; m) X. Zhu, Y. Xia, X. Zhang, A. A. Al-Khalaf, T. Zhao, J. Xu, L. Peng, W. N. Hozzein, W. Li, D. Zhao, *J. Mater. Chem. A* **2019**, *7*, 8975–8983; n) B. Wang, Y. Zhai, S. Li, X. Liu, T. Wang, C. Li, *J. Colloid Interface Sci.* **2020**, *574*, 122–130; o) Z. Luo, N. Wang, X. Pei, T. Dai, Z. Zhao, C. Chen, M. Ran, W. Sun, *J. Mater. Sci. Technol.* **2021**, *82*, 197–206; p) H. Yang, S. Kang, H. Zou, J. Jin, J. Ma, S. Li, *RSC Adv.* **2016**, *6*, 90462–90469.
- [9] a) M. Jiang, L. He, C. Duan, X. Ouyang, *Ceram. Int.* **2021**, *47*, 17520–17530; b) X. Li, Y. Liu, S. Wang, Y. Zhang, F. Liu, J. Han, *Colloids Surf. Physicochem. Eng. Aspects* **2021**, *631*, 127721; c) N. Xu, Y. Li, T. Zheng, L. Xiao, Y. Liu, S. Chen, D. Zhang, *Colloids Surf. Physicochem. Eng. Aspects* **2022**, *635*, 128085; d) S. Zhang, A. Hao, N. Nguyen, A. Oluwalowo, Z. Liu, Y. Dessureault, J. G. Park, R. Liang, *Carbon* **2019**, *144*, 628–638; e) L. Shanmugam, M. E. Kazemi, Z. Rao, D. Lu, X. Wang, B. Wang, L. Yang, J. Yang, *Compos. B. Eng.* **2019**, *178*, 107450; f) L. Shanmugam, X. Feng, J. Yang, *Compos. Sci. Technol.* **2019**, *174*, 212–220; g) G. Cai, S. Xiao, C. Deng, D. Jiang, X. Zhang, Z. Dong, *Corros. Sci.* **2021**, *178*, 109014; h) X. Jiang, M. Xi, L. Bai, W. Wang, L. Yang, H. Chen, Y. Niu, Y. Cui, H. Yang, D. Wei, *Mater. Sci. Eng. C* **2020**, *109*, 110553; i) C.-A. Xu, Z. Qu, H. Meng, B. Chen, X. Wu, X. Cui, K. Wang, K. Wu, J. Shi, M. Lu, *Polymer* **2021**, *223*, 123615; j) N. Taloub, L. Liu, N. Rahoui, M. Hegazy, Y. Huang, *Polym. Test.* **2019**, *75*, 344–349; k) C. Chen, G. Xiao, F. Zhong, S. Dong, Z. Yang, C. Chen, M. Wang, R. Zou, *Prog. Org. Coat.* **2022**, *162*, 106598.
- [10] a) Q. Han, A. Wang, W. Song, M. Zhang, S. Wang, P. Ren, L. Hao, J. Yin, S. Bai, *ACS Appl. Bio Mater.* **2021**, *4*, 6148–6156; b) M. Liao, P. Wan, J. Wen, M. Gong, X. Wu, Y. Wang, R. Shi, L. Zhang, *Adv. Funct. Mater.* **2017**, *27*, 1703852; c) Y. Wang, Y. Yu, J. Guo, Z. Zhang, X. Zhang, Y. Zhao, *Adv. Funct. Mater.* **2020**, *30*, 2000151; d) D. Xu, L. Sun, Z. Zhang, Y. Wang, X. Zhang, F. Ye, Y. Zhao, J. Pan, *Appl. Mater. Res.* **2021**, *24*, 101124; e) M. S. Sadi, J. Pan, A. Xu, D. Cheng, G. Cai, X. Wang, *Cellulose* **2019**, *26*, 7569–7579; f) Z.-G. Wang, Y.-L. Yang, Z.-L. Zheng, R.-T. Lan, K. Dai, L. Xu, H.-D. Huang, J.-H. Tang, J.-Z. Xu, Z.-M. Li, *Compos. Sci. Technol.* **2020**, *194*, 108190; g) Q. Guan, G. Lin, Y. Gong, J. Wang, W. Tan, D. Bao, Y. Liu, Z. You, X. Sun, Z. Wen, Y. Pan, *J. Mater. Chem. A* **2019**, *7*, 13948–13955; h) L. Zhang, J. He, Y. Liao, X. Zeng, N. Qiu, Y. Liang, P. Xiao, T. Chen, *J. Mater. Chem. A* **2019**, *7*, 26631–26640; i) L. Han, K. Liu, M. Wang, K. Wang, L. Fang, H. Chen, J. Zhou, X. Lu, *Adv. Funct. Mater.* **2018**, *28*, 1704195.
- [11] a) Q. Wu, N. Li, Y. Wang, Y. Liu, Y. Xu, S. Wei, J. Wu, G. Jia, X. Fang, F. Chen, X. Cui, *Biosens. Bioelectron.* **2019**, *144*, 111697; b) Z. Sun, H. Liu, X. Wang, *Biosens. Bioelectron.* **2022**, *195*, 113586; c) F. Chen, Q. Wu, D. Song, X. Wang, P. Ma, Y. Sun, *Colloids Surf. B. Biointerfaces* **2019**, *177*, 105–111; d) W.-Y. Jeon, H.-H. Kim, Y.-B. Choi, *Membranes* **2021**, *11*, 384; e) N. Wang, X. Zhao, H. Chen, L. Bai, H. Xu, W. Wang, H. Yang, D. Wei, L. Yang, *React. Funct. Polym.* **2020**, *154*, 104632.
- [12] a) D. Li, S. Li, J. Liu, L. Zhan, P. Wang, H. Zhu, J. Wei, *Mater. Sci. Eng. C* **2020**, *112*, 110887; b) H. Huang, M. Liu, D. Xu, L. Mao, Q. Huang, F. Deng, J. Tian, Y. Wen, X. Zhang, Y. Wei, *Mater. Sci. Eng. C* **2020**, *106*, 110157; c) T. Hu, M. Shi, X. Zhao, Y. Liang, L. Bi, Z. Zhang, S. Liu, B. Chen, X. Duan, B. Guo, *Chem. Eng. J.* **2022**, *428*, 131017; d) Y. Liang, X. Zhao, T. Hu, Y. Han, B. Guo, *J. Colloid Interface Sci.* **2019**, *556*, 514–528; e) K. Liu, L. Han, P. Tang, K. Yang, D. Gan, X. Wang, K. Wang, F. Ren, L. Fang, Y. Xu, Z. Lu, X. Lu, *Nano Lett.* **2019**, *19*, 8343–8356.
- [13] a) D. S. Su, S. Perathoner, G. Centi, *Chem. Rev.* **2013**, *113*, 5782–5816; b) V. Campisciano, M. Gruttadauria, F. Giacalone, *ChemCatChem* **2019**, *11*, 90–133; c) M. Melchionna, S. Marchesan, M. Prato, P. Fornasiero, *Catal. Sci. Technol.* **2015**, *5*, 3859–3875; d) S.-Y. Zhang, K. Yu, Y.-S. Guo, R.-Q. Mou, X.-F. Lu, D.-S. Guo, *ChemistryOpen* **2018**, *7*, 803–813; e) A. Ohtaka, J. M. Sansano, C. Nájera, I. Miguel-García, Á. Berenguer-Murcia, D. Cazorla-Amorós, *ChemCatChem* **2015**, *7*, 1841–1847.

- [14] a) V. Georgakilas, A. Bourlinos, D. Gournis, T. Tsoufis, C. Trapalis, A. Mateo-Alonso, M. Prato, *J. Am. Chem. Soc.* **2008**, *130*, 8733–8740; b) V. Georgakilas, A. Demeslis, E. Ntararas, A. Kouloumpis, K. Dimos, D. Gournis, M. Kocman, M. Otyepka, R. Zbořil, *Adv. Funct. Mater.* **2015**, *25*, 1481–1487.
- [15] X. Gu, W. Qi, X. Xu, Z. Sun, L. Zhang, W. Liu, X. Pan, D. Su, *Nanoscale* **2014**, *6*, 6609–6616.
- [16] A. Koutsioukis, V. Belessi, V. Georgakilas, *Green Chem.* **2021**, *23*, 5442–5448.
- [17] M. S. Strano, C. A. Dyke, M. L. Usrey, P. W. Barone, M. J. Allen, H. Shan, C. Kittrell, R. H. Hauge, J. M. Tour, R. E. Smalley, *Science* **2003**, *301*, 1519–1522.
- [18] a) J. L. Bahr, J. M. Tour, *Chem. Mater.* **2001**, *13*, 3823–3824; b) M. E. Lipińska, S. L. H. Rebelo, M. F. R. Pereira, J. A. N. F. Gomes, C. Freire, J. L. Figueiredo, *Carbon* **2012**, *50*, 3280–3294.
- [19] G. Yan, G. Chen, Z. Peng, Z. Shen, X. Tang, Y. Sun, X. Zeng, L. Lin, *Adv. Mater. Interfaces* **2021**, *8*, 2100239.
- [20] M. Schmidt, O. Benek, L. Vinklarova, M. Hrabínova, L. Zemanova, M. Chribek, V. Kralova, L. Hroch, R. Dolezal, A. Lycka, L. Prchal, D. Jun, L. Aitken, F. Gunn-Moore, K. Kuca, K. Musilek, *Int. J. Mol. Sci.* **2020**, *21*, 2059.
- [21] a) P. Salice, E. Fabris, C. Sartorio, D. Fenaroli, V. Figà, M. P. Casaletto, S. Cataldo, B. Pignataro, E. Menna, *Carbon* **2014**, *74*, 73–82; b) J. Pinson, F. Podvorica, *Chem. Soc. Rev.* **2005**, *34*, 429–439.
- [22] a) S. Eriksson, M. Boutonnet, S. Järås, *Appl. Catal. A* **2006**, *312*, 95–101; b) V. Campisciano, V. La Parola, L. F. Liotta, F. Giacalone, M. Gruttadauria, *Chem. Eur. J.* **2015**, *21*, 3327–3334; c) F. Giacalone, V. Campisciano, C. Calabrese, V. La Parola, Z. Syrgiannis, M. Prato, M. Gruttadauria, *ACS Nano* **2016**, *10*, 4627–4636.
- [23] H. Qian, Q. He, J. Zheng, S. Li, S. Zhang, *Polymer* **2014**, *55*, 550–555.
- [24] D. A. Shirley, *Phys. Rev. B* **1972**, *5*, 4709–4714.

---

Manuscript received: April 29, 2022  
Revised manuscript received: August 2, 2022  
Accepted manuscript online: August 2, 2022